JOURNAL OF Applied Polymer SCIENCE

Ag/Polyaniline Nanocomposites: Synthesize, Characterization, and Application to the Detection of Dopamine and Tyrosine

Bakhshali Massoumi,[1] Soghra Fathalipour,[1] Abdolhossein Massoudi,[1] Mohammad Hassanzadeh,[2] Ali Akbar Entezami

[1]Department of Chemistry, Payame Noor University, PO Box: 19395-3697, Tehran Iran
[2]Drug Applied Research Center, Tabriz University of Medical Sciences, Tabriz Iran
[3]Polymer Research Laboratory, Faculty of Chemistry, University of Tabriz, PO Box: 51666-16471, Tabriz Iran
Correspondence to: B. Massoumi (E-mail: b_massoumi@pnu.ac.ir)

ABSTRACT: In this research, Ag/Polyaniline (PANI) nanocomposites were synthesized successfully by the chemical oxidative polymerization of aniline in the presence of 4-aminothiophenol (4-ATP) capped colloidal Ag nanoparticles (NPs). First, Ag colloidal NPs were prepared by borohydride reduction of $AgNO_3$ in the presence of 4-ATP as a stabilizer. Then, polymerization of aniline in the presence of Ag NPs was carried out by ammonium persulfate as an oxidant at room temperature. TEM, SEM, XRD, FTIR, EDX, TGA, and UV–vis studies were done for the morphological, structural, thermal, and optical characterization of the Ag/PANI nanocomposite. Furthermore, Ag/PANI nanocomposites were immobilized on the surface of a glassy carbon electrode (GCE) and electroactivity behavior was investigated by cyclic voltammetry (CV) and differential pulse voltammetry (DPV). The obtained Ag/PANI modified GCE showed high catalytic activity for the oxidation of dopamine (DA) and tyrosine (Tyr). The peak current of differential pulse voltammograms of DA and Tyr increased linearly with their concentration in the ranges of 2.17–5.74 μM Tyr and 18.5–72.2 μM DA. The detection limits for DA and Tyr were 0.002 and 0.009 μM, respectively. © 2013 Wiley Periodicals, Inc. J. Appl. Polym. Sci. 000: 000–000, 2013

KEYWORDS: conducting polymers; colloids; composites; electrochemistry; nanostructured polymers

Received 14 February 2013; accepted 21 April 2013; Published online 00 Month 2013
DOI: 10.1002/app.39448

INTRODUCTION

Nanocomposites of conjugated conducting polymers and inorganic particles have attracted considerable academic and technological attention due to their unique physical properties and applications.[1,2] These hybrid nanomaterials are expected to exhibit several synergistic properties between the polymer and the metal nanoparticles, making them potential candidates for applications in numerous fields like biosensors,[3] sensors,[4] catalysis,[5] and memory devices.[6] The ability to control the shape and morphology of the nanocomposites is an important factor for defining their properties.[7,8]

Conducting polymers such as polypyrrole, polythiophene, and polyaniline have received much attention in the last two decades because of their potential use in various fields.[9] One of the notable features of conducting polymers is that it is possible to control the electrical conductivity of these polymers over a wide range from insulating to metallic by proper doping with suitable dopants.[10,11] Polyaniline (PANI) is one of the most important conducting polymers due to its high stability, ease of preparation, low monomer cost, high conductivity, different redox states, and a large variety of applications especially in light-emitting diodes, electronic devices, and chemical sensors.[12,13] On the other hand, metal nanoparticles such as silver (Ag) and gold (Au) have attracted much attention due to their unique physical high electrical and thermal conductivity, excellent surface-enhanced Raman scattering effect, chemical properties, electrocatalytic ability, and superior performance in technological fields.[14] The products containing silver nanoparticles have been commercially available for over 100 years and been utilized in applications as various as pigment, photography, wound treatment, conductive/antistatic composite, catalyst, nanosensor, and biocide.[15,16] As physical and chemical properties of these nanostructures depend on their size and shape, various approaches were developed to synthesize of non-agglomerated, uniform nanoparticles.[17–19] To obtain uniform nanoparticles with a well-controlled mean size and a narrow size distribution, it is necessary to use different capping molecules such as alkyl thiol, which binds on the surface of nanoparticles, and avoiding their aggregation.[20]

Applied Polymer SCIENCE

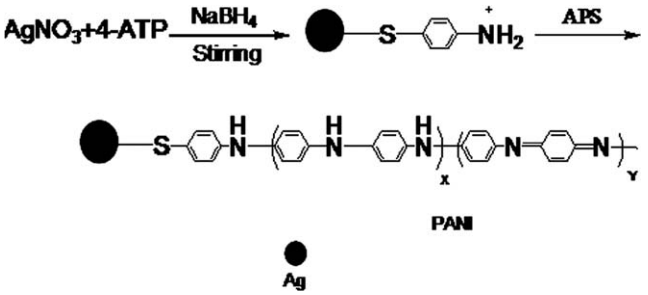

Scheme 1. Synthetic procedure for Ag/PANI nanocomposite.

Although many groups have synthesized polyaniline/silver nanocomposites by utilizing various methods, it is still a challenge to explore the various interesting properties of nanocomposites. For example, Gupta et al.[21] have synthesized PANI/Ag nanocomposites by polymerization of aniline in the presence of negatively charged silver nanoparticles. Khanna et al.[22] have prepared polyaniline/silver nanocomposites via *in situ* reduction of silver salt in aniline by mild photolysis. Shengyu et al.[23] have synthesized Ag/PANI core–shell nanocomposites successfully via *in situ* chemical polymerization of aniline based on mercaptocarboxylic acid capped Ag nanoparticles colloid. Sun et al.[24] have synthesized silver nanoparticles (NPs) using 4-ATP as stabilizer, and assembled the silver NPs onto the plasmid DNA through electrostatic interactions. To the best of our knowledge, this is a first report on synthesizing of silver/PANI nanocomposites through *in situ* polymerization of aniline in the presence of 4-ATP capped silver NPs. We selected 4-ATP capped silver nanoparticles because 4-ATP molecules act not only as capping agent but also amino groups of 4-ATP can be converted to cation radicals in the presence of oxidant, then polymerization continues with aniline to give Ag/PANI nanocomposites. On the basis of the excellent electrochemical behavior and catalytic property of PANI, it is reasonable to suggest that the resultant composites might be used to construct a kind of electrochemical sensor. Thus, the obtained Ag/PANI composite were immobilized on the surface of a glassy carbon electrode and it was found that the Ag/PANI modified electrode showed enhanced electrocatalytic activity for the oxidation of dopamine and tyrosine. The morphology, optical properties, thermal stability, and composition of the obtained Ag/PANI composites were characterized by scanning electron microscopy (SEM), transmission electron microscopy (TEM), energy-dispersive spectroscopy (EDX), ultraviolet visible spectroscopy (UV–vis), X-ray diffraction (XRD), Fourier transform infrared spectroscopy (FTIR), and thermogravimetric analysis (TGA).

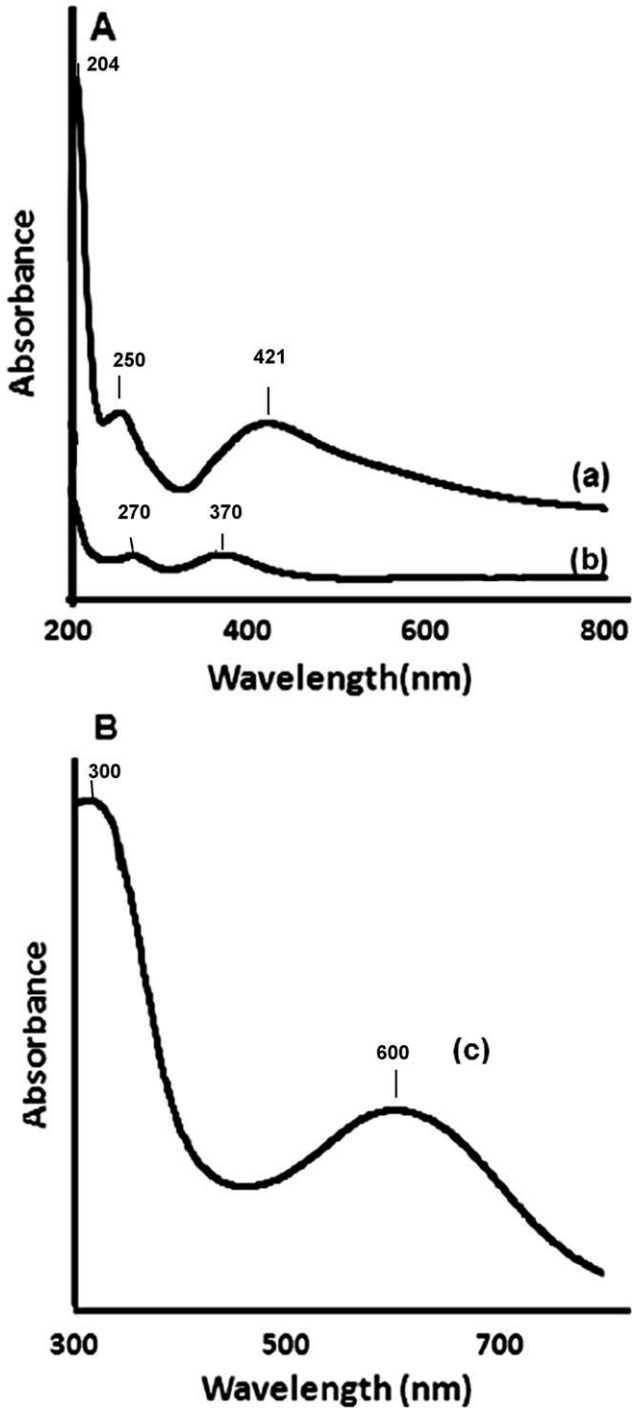

Figure 1. UV–vis spectrum of A: (a) 4-ATP capped Ag NPs colloid and (b) Ag/PANI nanocomposites dispersed in ethanol absolute and B: 4-ATP/PANI nanospheres dissolved in NMP.

EXPERIMENTAL

Materials and Methods

Aniline, ammonium persulfate ($(NH_4)_2S_2O_8$, APS), 4-aminothiophenol (4-ATP), hydrochloric acid (HCl), sodium borohydride ($NaBH_4$), silver nitrate, 1-methyl-2-pyrrolidone (NMP), tyrosine (Tyr), and dopamine (DA) were purchased from Merck. Aniline was distilled under reduced pressure and other reagents were used as received without further treatment. All solutions were prepared with deionized water.

Morphology and particle sizes of composites were noticed using by transmission electron microscopy (TEM, PHILIPS, CM10-HT, 100 kV) and morphology of the samples is also studied by a SEM (HITACHI, 4160) on Au substrate. X-ray diffraction patterns were taken on a SIEMENS (D5000) X-ray

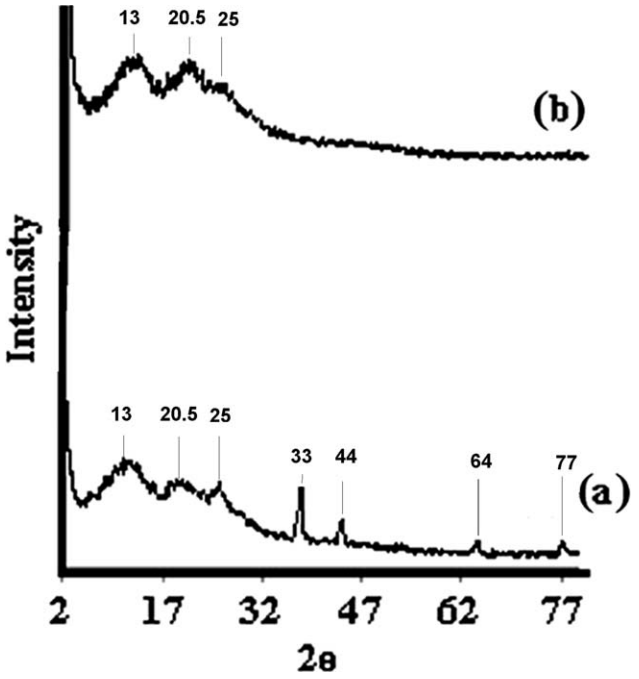

Figure 2. XRD pattern of (a) Ag/PANI nanocomposites and (b) 4-ATP/PANI nanospheres.

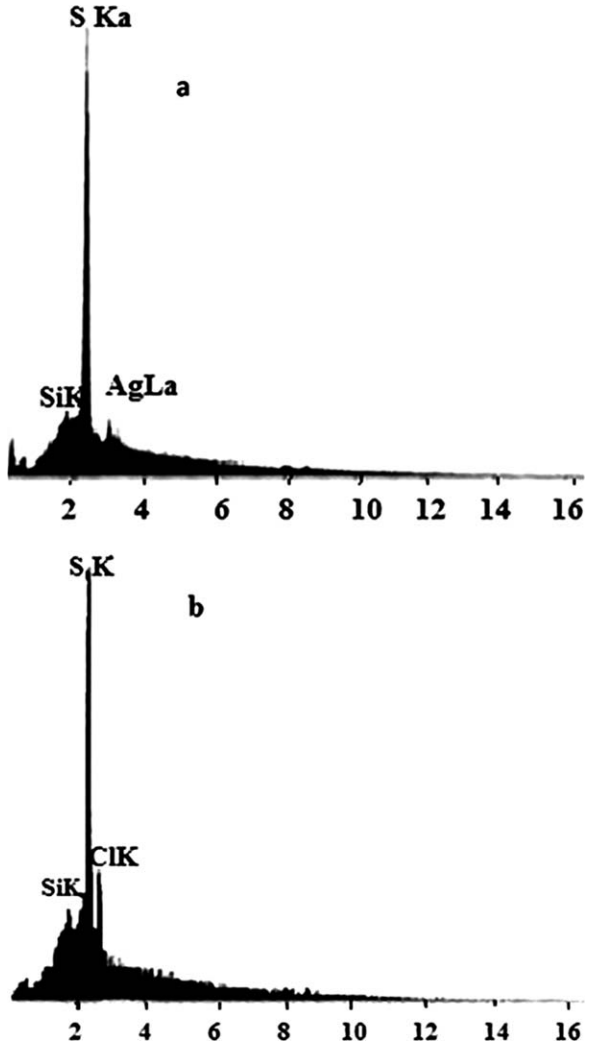

Figure 3. EDX analysis of (a) Ag/PANI nanocomposites and (b) 4-ATP/PANI nanospheres.

diffractometer with Cu $K\alpha$ radiation, at a 10°/min scanning speed from 2° to 90° (in 2θ). Ultraviolet visible (UV–vis) absorption spectra were taken using a SHIMADZU (UV-1601PC) spectrophotometer. Nanocomposites were dispersed in ethanol and 4-ATP/PANI was dissolved in NMP. All Fourier transform infrared (FTIR) spectroscopic measurements were performed on a Bruker model Tensor Fourier transform spectrometer in the range of 400–2000 cm^{-1} using KBr pressed disks. Thermogravimetric analysis (TGA) was carried out on a METTLER-TOLEDO-(TGA/SDTA 851) instrument from 50–800°C with a heating rate of 10°C min^{-1} in N_2 atmosphere. The electrical conductivity of the samples was measured by a standard four-probe method on pressed pellets of samples prepared at the room temperature using an Azar Electric Co. instrument (Iran). Electrochemical experiments were conducted using Autolab instrument (PGSTATE12) in a three-electrode system. All electrochemical experiments were performed in a cell containing 20 mL of phosphate buffer solution (PBS, 0.1*M*) at room temperature and using platinum wire as the auxiliary, a saturated calomel electrode (SCE) as the reference, and the Ag/PANI modified glassy carbon electrode (GCE) as the working electrode. All experimental solutions were deaerated by bubbling highly pure nitrogen for 10 min, and a nitrogen atmosphere was kept over the solutions during electrochemical measurements.

Synthesis of Ag Nanoparticles

4-ATP capped silver nanoparticles were prepared in a water-ethanol system according to the literature.[24] A 2 mL 4-ATP ethanol solution (1 m*M*) was injected dropwise to 20 mL silver nitrate (0.5 m*M*) solution under vigorous stirring. After the dissolution of 4-ATP, 0.4 mL of freshly prepared aqueous sodium borohydrid solution (10 m*M*) was injected dropwise into the solution under vigorous stirring. Then, the silver clear black brown colloids were centrifuged twice at 5000 rpm for 20 min and the obtained precipitates were removed by centrifuging.

Synthesis of Ag/PANI Nanocomposites

The Ag/PANI nanocomposites were synthesized by *in situ* chemical polymerization in the following manner: 0.2 g (2.1×10^{-3}mol) of aniline was added to Ag NPs colloid solution, keeping the molar ratio of $AgNO_3$ to aniline as 1 : 100. After the dissolution of aniline, 0.46 g (2.1×10^{-3}mol) of ammonium persulfate as oxidant was added to reaction mixture and maintained under magnetic stirring for 20 h at the room temperature. The product was filtered and thoroughly washed with deionized water and methanol to remove non-reacted monomer, oligomer, and excess of oxidant until the filtrate turned colorless. Obtained composites were dried in vacuum at 40°C for 24 h.

Synthesis of 4-ATP/PANI Nanospheres

For comparison, 4-ATP/PANI nanospheres were synthesized according to a similar procedure used for Ag/PANI

Applied Polymer SCIENCE

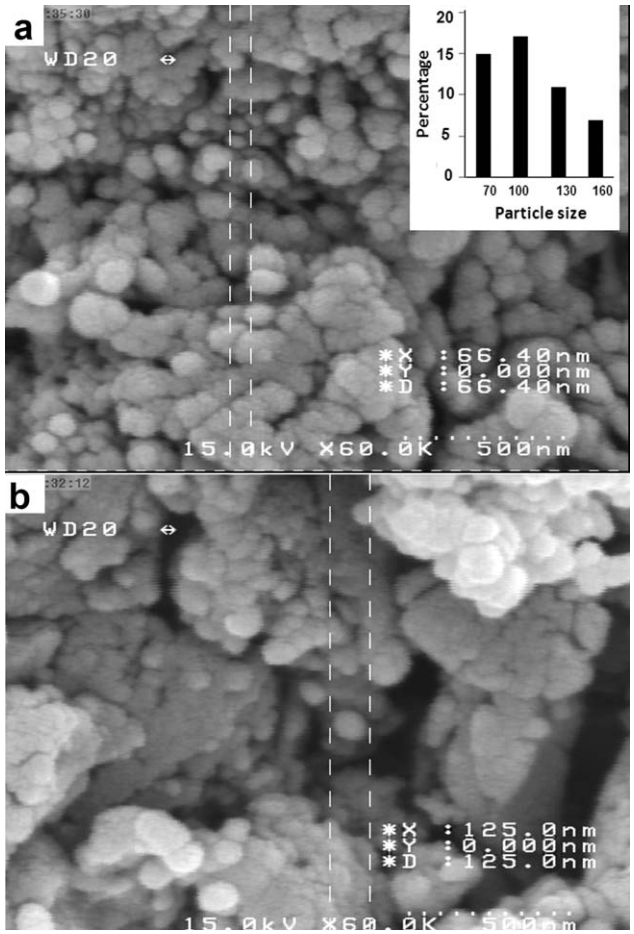

Figure 4. SEM images of (a) 4-ATP/PANI nanospheres and size distribution of 4-ATP/PANI nanospheres (inset), and (b) Ag/PANI nanocomposites.

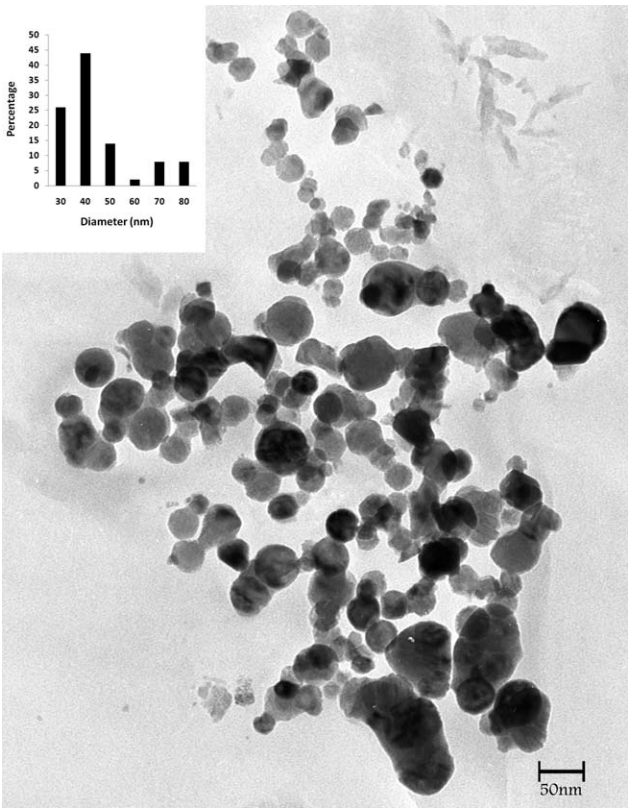

Figure 5. TEM images of Ag/PANI nanocomposites. Size distribution of Ag/PANI nanocomposites (inset).

nanocomposites. A 2 mL of 4-ATP ethanol solution (1 m*M*) was added to 20 mL deionized water and it was adjusted at pH: 3.5 with HCl solution (0.1*M*), then was added 0.2 g (2.1×10^{-3}mol) of aniline and 0.46 g (2.1×10^{-3}mol) of APS, respectively. The mixture of reaction was maintained under magnetic stirring for 20 h at the room temperature. The product was filtered and washed with deionized water and methanol, then was dried in vacuum at 40°C for 24 h.

Preparation of Ag/PANI Modified Glassy Carbon Electrode

The glassy carbon electrode (GCE) was polished with alumina slurry followed by a rinse with deionized water and then allowed to dry at the room temperature. Ag/PANI were dispersed in distilled water to form a 2.0 mg/mL solution, and then 5 μL of colloidal solution was dropped onto the pre-treated GCE surface and allowed to dry under ambient conditions.

RESULTS AND DISCUSSION

Synthesis and Characterization of Ag/PANI Nanocomposites and 4-ATP/PANI Nanospheres

Ag coated PANI nanocomposites were successfully synthesized through *in situ* polymerization in the presence of 4-ATP caped silver nanoparticles. The synthesis procedure and possible mechanism for formation of Ag/PANI nanocomposites is shown in Scheme 1. 4-ATP not only acted as an anchor agent, but also prevented the aggregation of PANI efficiently. The prepared solution of silver nanoparticles displayed a weak acidity, so it was possible that the free amino was positively charged. 4-ATP molecules with reactive terminal groups (NH_3^+) acted as ligands which were highly prone to oxidation.[25] 4-ATP radical cations acted as a point of nucleation to initiate the polymerization reaction of aniline monomer leading to the formation of the core–shell structure. The concentration of silver nitrate, 4-ATP ethanol solution, the reaction time, the velocity and time of centrifuge had fundamental effect on the stability of 4-ATP capped silver nanoparticles.[24] In polymerization of aniline in presence of Ag NPs, with the addition of HCl aqueous solution of ammonium persulfate to mixture, a colorless solution was appeared that gradually turned blue. Although the amine groups of 4-ATP are almost fully ionized at pH lower than 3 but the silver nanoparticles is easier to flocculate under such conditions.[26] Therefore, polymerization of PANI was carried out in the presence of positively charged silver nanoparticles without the addition of acid.

Figure 1 shows the UV–vis absorption spectra of Ag NPs, Ag/PANI nanocomposites, and undoped 4-ATP/PANI nanospheres [Figure 1(A,B)]. 4-ATP-stabilized colloidal Ag NPs exhibit absorption peaks at 204, 250, and 421 nm which are related to n–π^*, π–π^* and surface Plasmon resonance (SPR), respectively [Figure 1(A-a)].[27] It is well known that the SPR bands of metal nanoparticles are sensitive to a number of factors, such as particle size, shape, and the nature of the

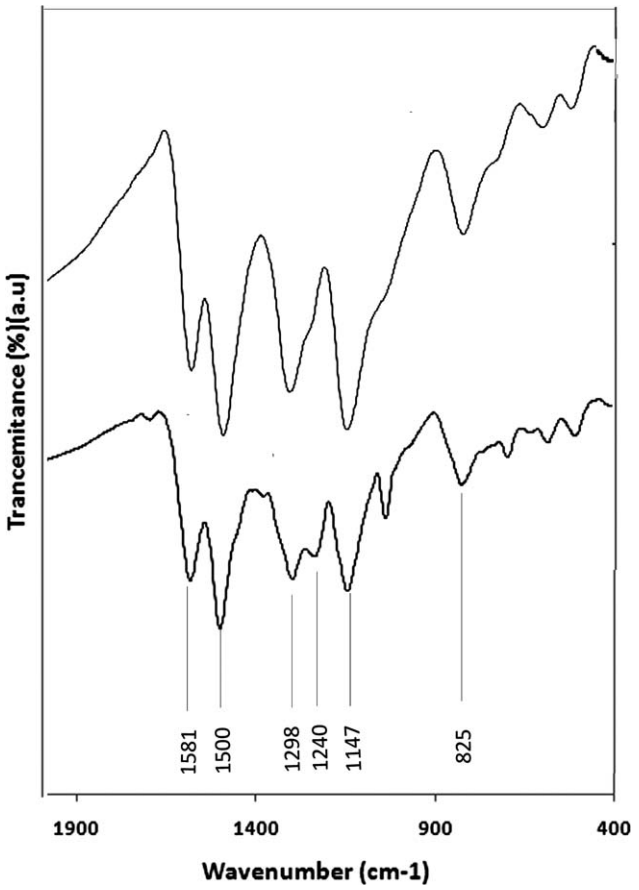

Figure 6. FT-IR spectrum of (a) 4-ATP/PANI nanospheres and (b) Ag/PANI nanocomposites.

surrounding media.[28] Characteristic peaks of Ag/PANI nanocomposites were appeared at 270 and 370 nm which are attributed to π–π^* transitions [Figure 1(A-b)].[23] In Figure 1(A-b), the characteristic peaks for the polaron–π^*, π–polaron transitions of polyaniline and the SPR peak of the Ag NPs are absent [Figure 1(A-b)] which this could be related to the strong interaction between Ag NPs and PANI.[29] The characteristic peaks of 4-ATP/PANI were appeared at 300 and 600 nm that shows PANI is in an undoped state [Figure 1(B-c)].[30]

The X-ray diffraction patterns of the Ag/PANI nanocomposites and 4-ATP/PANI nanospheres are shown in Figure 2. In XRD pattern of the Ag/PANI nanocomposites [Figure 2(a)], diffraction peaks at $2\theta = 13°$, 20.5°, and 25° are ascribed to the periodicity parallel and perpendicular of the PANI chains, respectively.[31] Another four diffraction peaks at 38°, 44°, 64°, and 77° are related to (1 1 1), (2 0 0), (2 2 0), and (3 1 1) Bragg's reflection of silver structure.[14] XRD patterns of NPs show several different size-dependent features leading to anomalous peak positions, heights, and widths.[32–34] The average particle sizes (D) were calculated from the Ag (1 1 1) diffraction line using Scherrer's equation, $D = k\lambda/\beta \cos\theta$, where k is particle shape factor (generally taken as 0.89), λ is the wave length of Cu $K\alpha$ radiation ($\lambda = 1.54$ Å), θ is the diffraction angle, and β is the full width at half maximum (FWHM) of the diffraction peak.[23] The calculated average size of silver is about 26 nm (FWHM = 0.326°), which is consistent with the result of the TEM. These results confirmed the presence of Ag NPs in resulted Ag/PANI nanocomposites. The XRD pattern of PANI nanospheres shows characteristic peaks of polymer chains at 2θ = 13°, 20.5°, and 25° [Figure 2(b)].

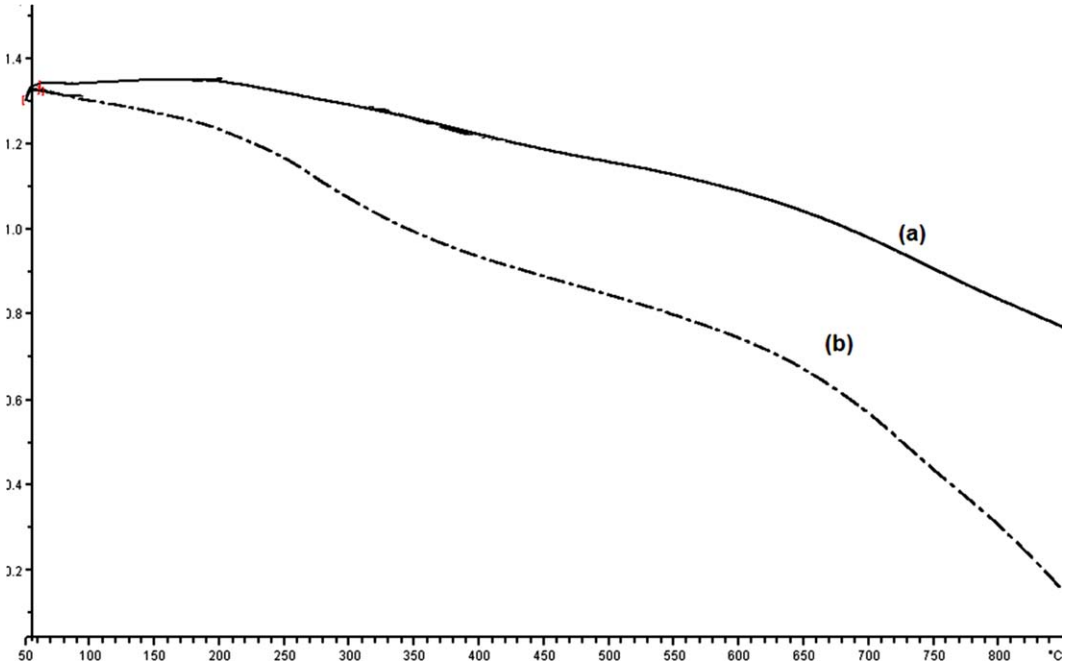

Figure 7. TGA thermograms of (a) 4-ATP/PANI nanospheres and (b) Ag/PANI nanocomposites. [Color figure can be viewed in the online issue, which is available at wileyonlinelibrary.com.]

Applied Polymer SCIENCE

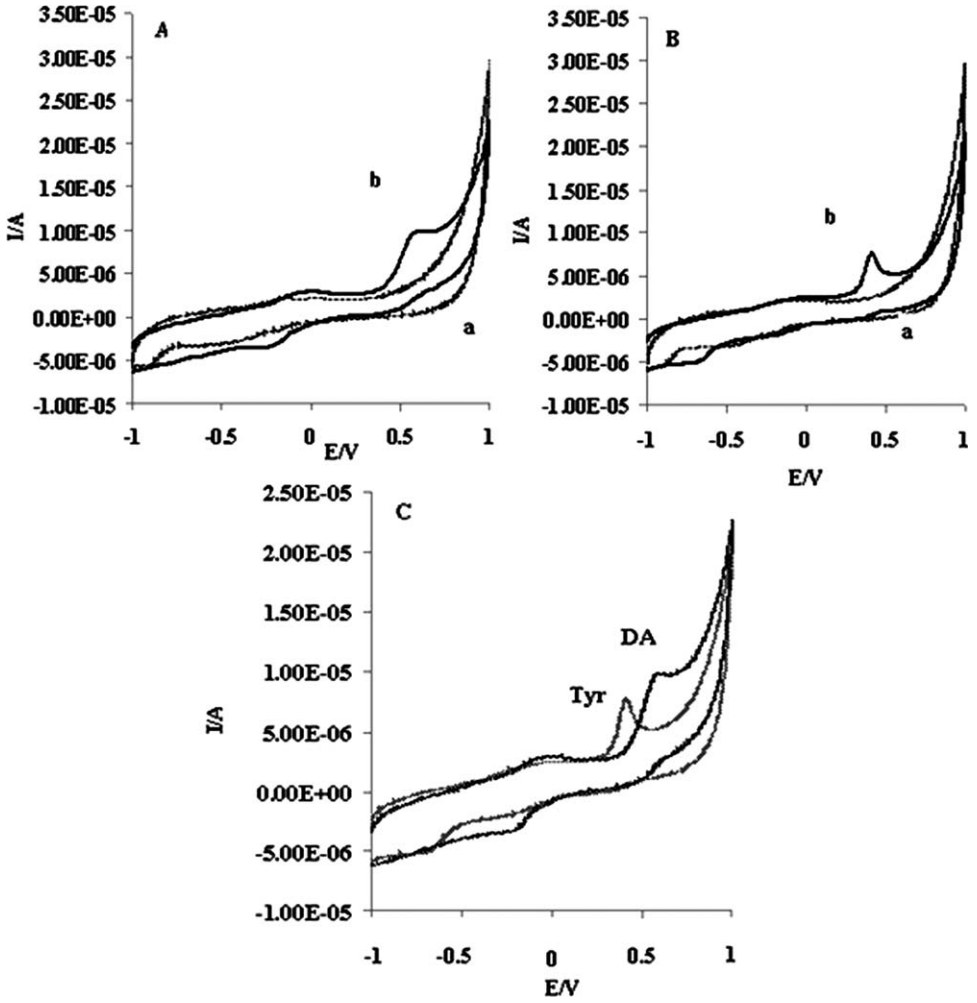

Figure 8. A: Cyclic voltammograms of the (a) Ag/PANI/GC in the absence and (b) presence of 30 μM of DA. B: Cyclic voltammograms of the (a) Ag/PANI/GC in the absence and (b) presence of 50 μM of Tyr. C: Cyclic voltammograms of 30 μM DA and 50 μM Tyr at surface of Ag/PANI/GC. Scan rate is 50 mV s^{-1}.

The elemental compositions of the Ag/PANI nanocomposites and 4-ATP/PANI nanospheres are shown by EDX analysis in Figure 3(a) and (b), respectively. The presence of silver and sulfur were confirmed by selected area EDX studies.

Figure 4 shows the morphology of the 4-ATP/PANI [Figure 4(a)] and Ag/PANI nanocomposites [Figure 4(b)]. From the SEM image, it is observed that 4-ATP/PANI display sphere morphology with average particle size ranges between 50 and 160 nm with the maximum close to 100 nm [Figure 4(a), inset]. Also from Figure 4(b), it can be seen that Ag/PANI nanocomposites display fused sphere morphology.

Figure 5 shows the TEM image [Figure 5(a)] and histogram of particle size distribution of Ag/PANI [Figure 5(b)]. Core–shell nanocomposites and PANI nanospheres were shown in TEM image of Ag/PANI nanocomposites [Figure 5(a)]. The TEM image shows that in core–shell structure, the Ag nanoparticles with a mean diameter of *ca.* 25 nm are the cores of the nanocomposites and the polyaniline as the shell wraps of the Ag nanoparticles. The graph [Figure 5(b)] shows that average particle size ranges between 20 and 90 nm with the maximum close to 40 nm.

Figure 6 shows the FT-IR spectra of Ag/PANI nanocomposites and 4-ATP/PANI nanospheres in 400 to 4000 cm^{-1} region. The FT-IR measurement of 4ATP/PANI represents peaks at 1581 and 1500 cm^{-1} correspond to C=C stretching of the quinoid and benzoid rings, respectively [Figure 6(a)]. The characteristic bands at 1298 and 1240 cm^{-1} represent C–N and C=N stretching modes, respectively. The absorption peak at 1147 cm^{-1} is assigned to the in-plane bending of C–H, and the peak at 825 cm^{-1} is attributable to C–H bending vibration out of the plane of the para-disubstituted benzene rings.[35] The infrared spectrum of the Ag/PANI nanocomposites is similar to the 4-ATP/PANI and confirms the formation of PANI in composites.

Thermal stability testing was carried out using TGA. Figure 7 shows a comparison of the mass losses between 4ATP/PANI nanospheres [Figure 7(a)] and Ag/PANI nanocomposites [Figure 7(b)]. In Figure 7(a,b), the initial mass loss is due to the loss of water molecules, the next mass loss may be attributed

to the loss of oligomer and the subsequent mass loss occurred due to the degradation of the polymer chain.[36] Rapid mass loss occurs at around 600°C due to rapid degradation of polymer chain.[37] The remaining masses of 4ATP/PANI nanospheres and Ag/PANI nanocomposites at 800°C are 59and 11%, respectively. The inferior thermal stability of Ag/PANI composites is due to the presence of Ag–S covalent bond in their structure.

Electrical conductivity of 4-ATP/PANI nanospheres and Ag/PANI nanocomposites was measured by a standard four-probe method. The electrical conductivity of 4-ATP/PANI nanospheres (5.69 S cm^{-1}) was higher than conductivity of Ag/PANI nanocomposites (1.74 S cm^{-1}). This can be justified considering the fact that during the synthesis of the composite, solution of silver nanoparticles was added which provides a reducing atmosphere. This is further supported by the fact that a higher amount of oxidizing agent is required during the synthesis of Ag/PANI composites. Due to these reasons, polyaniline in Ag/PANI is in a relatively reduced state as compared to 4ATP/PANI nanospheres.[38] It is a well known fact that the conductivity of polyaniline is highly dependent on the oxidation state of the polymer and that the half oxidized emeraldine salt form is the conducting state of polyaniline.[37]

Electrocatalytic Oxidation and Determination of Dopamine and Tyrosine Using Ag/PANI Nanocomposites

Dopamine (DA), a simple organic chemical in the catecholamine family, is an important neurotransmitter in mammalian brain system that is responsible for reward-driven learning, and the loss of DA-containing neurons may cause serious diseases such as Parkinson. Tyrosine (Tyr) is a non-essential amino acid used by cells to synthesize proteins and dopamine can be produced from tyrosine metabolism. Therefore, the detection of DA and Tyr has been a subject of significant interest. PANI shows good electrochemical behavior and are applied to the field of chemically modified electrodes. In this study, Ag/PANI nanocomposites were immobilized onto the surface of a glassy carbon electrode (GCE), which leads to the efficient electrocatalytic oxidation of DA and Tyr. The GCE was previously tested in PBS buffer (pH = 3) before nanocomposites were drop coated on it. It presented no redox process in the potential range applied. The working electrode coated with Ag/PANI nanocomposites was immersed in the electrolyte solution for 20 min prior to the measurement to ensure the diffusion of the solution to the interlayer space and permit better ionic exchange.

The cyclic voltammograms were recorded for DA and Tyr at Ag/PANI electrode and are shown in Figure 8. As it can be seen, at the surface of the modified electrode, oxidations of DA and Tyr are irreversible processes. These results indicate that the electron transfer rate is quite slow. Such sluggish electron transfer kinetics is due to the electrode fouling caused by the deposition of DA and Tyr and their oxidation products.

In addition, at modified electrode, oxidation of these compounds resulted in a typical electrocatalytic response. Also, in the presence of DA and Tyr, it was observed that the anodic current and the

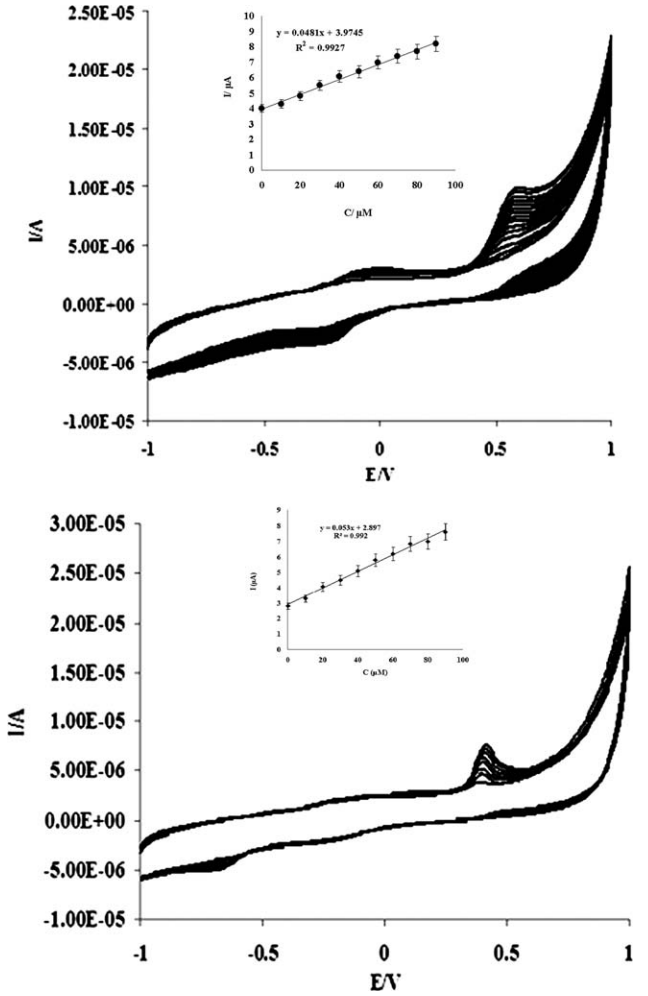

Figure 9. A: Cyclic voltammograms of Ag/PANI/GC in the presence of different concentrations of DA. The potential scan rate is 50 mV s^{-1}. Inset: dependence of the anodic current electro-oxidation on DA concentration in the range of 10–80 μM. B: Cyclic voltammograms of Ag/PANI/GC in the presence of different Tyr concentrations. The potential scan rate is 50 mV s^{-1}. Inset: dependency of the anodic current electro-oxidation on Tyr concentration in the range of 10–130 μM.

associated anodic charge increased drastically, while the cathodic current and the corresponding charge decreased.

Figure 9(A) and (B) show that upon increasing DA and Tyr concentration its irreversible oxidation develops in the region of the electrochemical formation of Ag/PANI. It is observed that any increase in the concentration of compounds causes a proportional almost linear enhancement of the anodic wave [Figure 9(A,B)]. It is observed that in the presence of DA and Tyr the anodic current increases while the cathodic current decreases and the charges associated with the processes also behave accordingly to the extent of 17.03 and 20.98%, respectively. The tolerance limit was defined as the molar ratio of the additive/drugs causes an error less than 5.1 and 4.4% for determination of 30 and 50 μM DA and Tyr, respectively.

The differential pulse voltammograms (DPV) recorded for DA and Tyr at modified electrode is shown in Figure 10. The DPVs

Applied Polymer SCIENCE

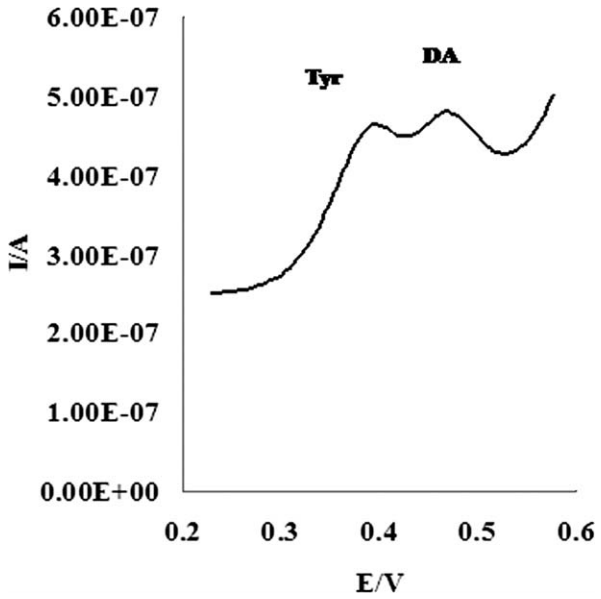

Figure 10. Differential pulse voltammograms of 0.0114 μM Tyr, and 0.0176 μM DA at Ag/PANI/GC.

of DA and Tyr at modified electrode show excellent improvement in oxidation peak currents for DA and Try. Therefore, DA and Tyr could be more accumulated on the electrode surface. Consequently, Figure 10 indicates that the application of Ag/PANI leads to enhance of current sensitivity and selectivity in simultaneous detection of DA and Tyr.

To verify the linear relationship between anodic peak currents Tyr and DA concentrations, several calibration curves were constructed under optimum conditions. Figure 11 shows differential pulse voltammograms obtained at Ag/PANI in various concentrations of Tyr and DA. A linear dynamic range with a calibration equation of Ip (μA) = 0.005c (μM) + 0.3618 (R^2 = 0.9934), and a detection limit of 0.002 μM (S/N = 3) was obtained for DA. A linear relationship was found for Tyr with a calibration equation of Ip (μA) = 0.0338c (μM) + 0.3668 (R^2 = 0.9966) and a detection limit of 0.009 μM [Figure 11(B)].

The results obtained by this modified electrode are compared in Table I with previously reported modified electrode.[38–46] Ag/PANI/GC is different from other reported electrodes such as: simplicity and low cost construction, LOD, selectivity, and linear range. In terms of LOD, the proposed sensor posses an LOD of 1.4 and 2.1 μM for Tyr and DA, respectively, whereas other electrode provided lower LODs. But Ag/PANI/GC provided wide linear range for detection of these molecules. Generally, it could be seen that the Ag/PANI/GC offered reasonable linear ranges for Tyr and DA detections and the detection limit was lower than some of previous reports. These results indicate that Ag/PANI/GC is an appropriate platform for the determination of Tyr and DA. With the manufacture of more Tyr and DA electrochemical sensors, it was found that Tyr and DA have lower detection potentials on Ag/PANI/GC which is important in practical chemical analyses. Therefore, the detection of Tyr and DA by Ag/PANI/GC is appropriate.

The repeatability of the modified electrode was investigated by recording CVs in different immerse time of electrode on

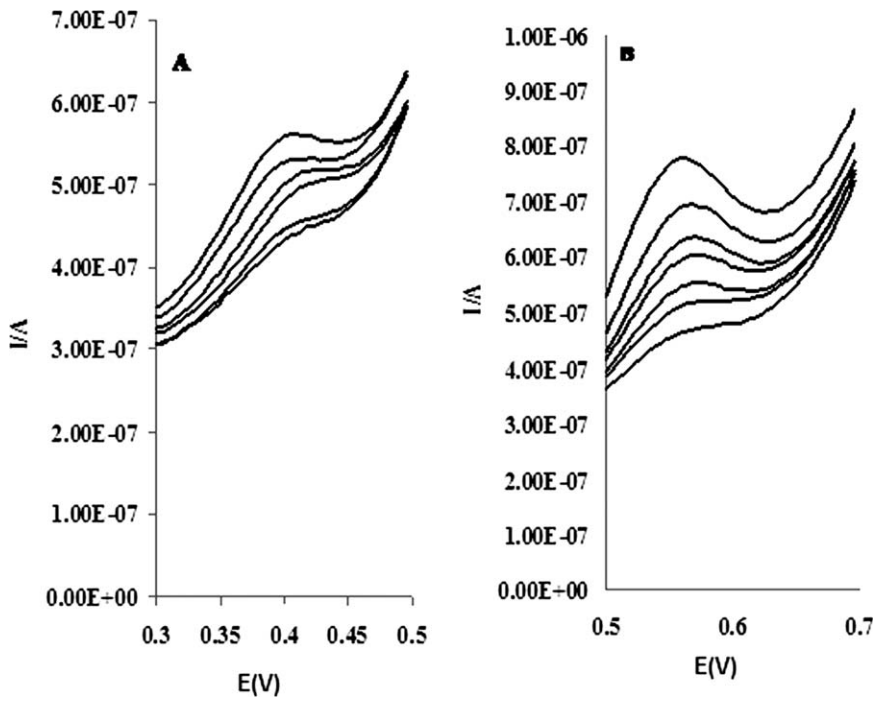

Figure 11. A and B: Differential pulse voltammograms of Ag/PANI/GC in different concentrations of Tyr and DA, respectively.

Table I. Analytical Parameters for Detection of Tyr and DA at Previously Reported Methods

Type of analyte	Sensor	Method	Linear range	LOD	References
Tyr	Cobalt hydroxide/GC	DPV	13–6000 nM	5.21 nM	39
	Fe (III)-Schiff base complexes modified CN/GC	DPV	8–1308 nM	10.03 nM	40
	MCM-41-NH_2/GC	FIA	405–1015 nM	56.03 nM	41
	Gold nanoparticle/cystamine/GC	Amperometry	0.1–300 nM	0.04 nM	42
	Ag/PANI/GC	DPV	-	9 nM	This work
DA	Boron-doped CNT/GCE	DPV	20–7500 μM	1.4 μM	43
	MCNT-poly(DBA)/GCE	Amperometry	10–70 nM	0.1 nM	44
	EDTA-GS/Nafion/GCE	CV	0.2–25 nM	0.1 nM	45
	PTCA-GS/MCNT/IL/GCE	Amperometry	30–3800000 nM	1.2 nM	46
	Ag/PANI/GC	DPV	-	2 nM	This work

buffer solution. When the modified electrode was stored in buffer solution for different time (10–80 min), the current response decreased 2.5% after about 80 min. Furthermore, the current response of the modified electrode in buffer solution, after 100 rounds of cyclic scanning was almost unchanged. It proved the good stability of the modified electrode. The GC electrode modified with polymer nanocomposite imparts a higher stability onto voltammetric measurements of analyte.

CONCLUSION

In summary, we synthesized Ag/PANI nanocomposites via in situ chemical oxidation polymerization of aniline based on 4-ATP capped silver nanoparticles. TEM and SEM images confirm the formation of core/shell Ag/PANI composites and PANI nanospheres. The presence of Ag nanoparticles in resulted nanocomposites could be observed from XRD and EDX analysis. The diameter of Ag/PANI nanocomposites obtained from XRD and TEM was around 40 nm. TGA results indicated that 4-ATP/Polyaniline nanospheres were more thermally stable than Ag/PANI nanocomposites. Furthermore, this kind of nanocomposites was applied to the preparation of a new chemically modified electrode. The Ag/PANI modified electrode showed enhanced electrocatalytic activity for the oxidation of DA and Ty. The nanocomposites may have potential application in biological separation, enzyme immobilization, and biosensors.

REFERENCES

1. Ward, R. E.; Meyer, T. Y. *Macromolecules* **2003**, *36*, 4368.
2. Huang, J.; Moore, J. A.; Acquaye, J. H.; Kaner, R. B. *Macromolecules* **2005**, *38*, 317.
3. Tian, S.; Liu, J.; Zhu, T.; Knoll, W. *Chem. Mater.* **2004**, *16*, 4103.
4. Majumdar, G.; Goswami, M.; Sarma, T. K.; Paul, A.; Chatto, P. A. *Langmuir* **2005**, *21*, 1663.
5. O'Mullane, A. P.; Dale, S. E.; Macpherson, J. V.; Unwin, P. R. *Chem. Commun.* **2004**, *14*, 1606.
6. Tseng, R. J.; Huang, J.; Ouyang, J.; Kaner, R. B.; Yang, Y. *Nano. Lett.* **2005**, *5*, 1077.
7. Alivisatos, A. P. *Science* **1996**, *271*, 933.
8. Huang, J.; Kaner, R. B. *J. Am. Chem. Soc.* **2004**, *126*, 851.
9. Roy, B. C.; Gupta, M. D.; Bhowmik, L.; Ray, J. K. *Bull. Mater. Sci.* **2001**, *24*, 389.
10. Wang, H. L.; MacDiarmid, A. G.; Wang, Y. Z.; Gebler, D. D.; Epstein, A. J. *Synth. Met.* **1996**, *78*, 33.
11. Mirmohseni, A.; Wallace, G. G. *Polymer*, **2003**, *44*, 3523.
12. Griesser, T.; Radl, S. V.; Koepplmayr, T.; Wolfberger, A.; Edler, M.; Pavitschitz, A.; Kratzer, M.; Teichert, C.; Rath, T.; Trimmel, G.; Schwabegger, G.; Simbrunner, C.; Sitter, H.; Kern, W. *J. Mater. Chem.* **2012**, *22*, 2922.
13. Huang, J.; Virji, S.; Weiller, B. H.; Kaner, R. B. *J. Am. Chem. Soc.* **2003**, *125*, 314.
14. Sun, Y.; Xia, Y. *Adv. Mater.* **2002**, *14*, 833.
15. Bernd, N.; Harald, F.; Murray, H. *Environ. Sci. Technol.* **2011**, *45*, 1177.
16. Jin, R.; Cao, Y. W.; Mirkin, A.; Kelly, K. L.; Schatz, G. C.; Zhang, J. G. *Science* **2001**, *294*, 1901.
17. Brust, M.; Kiely, C. *Colloids. Surf. A.* **2002**, *202*, 175.
18. Pileni, M. P. *Appl. Surf. Sci.* **2001**, *171*, 1.
19. Jana, N. R.; Gearheart, L.; Murphy, C. J. *Langmuir* **2001**, *17*, 6782.
20. Oliveria, M. M.; Zanchet, D.; Ugarte, A. J.; Zarbin, G. *J. Colloid. Interf. Sci.* **2005**, *292*, 429.
21. Gupta, K.; Jana, P. C.; Meikap, A. K. *Synth. Met.* **2010**, *160*, 1566.
22. Khanna, P. K.; Singh, N.; Charan, S.; Viswanath, A. K. *Mater. Chem. Phys.* **2005**, *92*, 214.
23. Shengyu, J.; Shuangxi, X.; Lianxiang, Y.; Yan, W.; Chun, Z. *Mater. Lett.* **2007**, *61*, 2794.
24. Sun, L.; Wei, G.; Song, Y.; Liu, Z.; Wang, L.; LiZhuang, Z. *Appl. Surf. Sci.* **2006**, *252*, 4969.

25. Perera, G.; Hombach, J.; Bernkop, S. A. *AAPS Pharm. Sci. Tech.* **2010**, *11*, 174.

26. Dong, A. G.; Wang, Y. J.; Tang, Y.; Ren, N.; Yangb, W. L.; Gaoa, Z. *Chem. Commun.* **2002**, *4*, 350.

27. zhang, J. H.; Liu, K.; Cui, Z. C.; Zhang, G.; Zhao, B.; Yang, B. *J. Colloid. Interf. Sci.* **2002**, *255*, 115.

28. Buffat, P. A. *Mater. Chem. Phys.* **2003**, *81*, 368.

29. Yu, Q., Shi, M.; Cheng, Y.; Wang, M.; Chen, H. Z. *Nanotechnology* **2008**, *19*, 265702.

30. Ayad, M. M.; Prastomo, N.; Matsuda, M.; Stejskal, J. *Synth.. Met.* **2010**, *160*, 42.

31. Pouget, J. P.; Jozefowicz, M. E.; Epstein, A. J.; Tang, X.; MacDiarmid, A. G. *Macromolecules* **1991**, *24*, 779.

32. Hall, B. D. *J. Appl. Phys.* **2000**, *87*,1666.

33. Buffat, P. A. *Mater. Chem. Phys.* **2003**, *81*, 368.

34. Lee, J. W.; Stein, G. D. *J. Phys. Chem.* **1987**, *91*, 2450.

35. Paulraj, P.; Janaki, N.; Sandhya, S.; Pandian, K. *Colloids. Surf. A* **2011**, *377*, 28.

36. Palaniappan, S.; Narayana, B. H. *Polym. Sci. A: Polym. Chem.* **1994**, *32*, 2431.

37. Gupta, K.; Jana, P. C.; Meikap, A. K. *Synth. Met.* **2010**, *160*, 1566.

38. Prabhakar, P. K.; Raj, S.; Anuradha, P. R.; Sawant, S. N.; Doble, M. *Colloids Surf. B.* **2011**, *86*, 146.

39. Hasanzadeh, M.; Karim-Nezhad, G.; Shadjou, N.; Khalilzadeh, B.; Saghatforoush, L. A.; Abnosi, M. H.; Ershad, S. *Anal. Biochem.* **2009**, *389*, 130.

40. Saghatforoush, L. A.; Hasanzadeh, M.; Shadjou, N.; Khalilzadeh, B. *Electrochim. Acta* **2011**, *56*, 1051.

41. Hasanzadeh, M.; Shadjou, N.; Chen, S. T.; Sheykhzadeh, P. *Catal. Commun.* **2012**, *19*, 21.

42. Deo, R. P.; Lawrence, N. S.; Wang, J. *Analyst* **2004**, *129*, 1076.

43. Deng, C. Y.; Chen, J. H.; Wang, M. D.; Xiao, C. H.; Nie, Z.; Yao, S. Z. *Biosens. Bioelectron.* **2009**, *24*, 2091.

44. Zhou, X.; Zheng, N.; Hou, S. R.; Li, X. J.; Yuan, Z. B. *J. Electroanal. Chem.* **2010**, *642*, 30.

45. Hou, S. F, Kasner, M. L.; Su, S. J.; Patel, K.; Cuellari, R. *J. Phys. Chem. C* **2010**, *114*, 14915.

46. Niu, X.; Yang, W.; Guo, H.; Ren, J.; Gao, J. *Biosens. Bioelectron.* **2013**, *41*, 225.